Chemical Process Design Vol.3 No.2 (2024) 34-51

University of Sistan and Baluchestan

Chemical Process Design

Available online at http://cpd.usb.ac.ir/

Spiral Heat Exchanger's Mathematical Modelling and Optimization using Multipurpose Genetic Algorithm

Mehdi Jafari[1], Jamshid Khorshidi[2,*], Ali Sheibani[1], Taleb Zarei[2]

[1]Department of Chemical Engineering,Yazd Branch, Islamic Azad University, Yazd, Iran
[2]Department of Mechanical Engineering, University of Hormozgan, Bandar Abbas, Iran

ARTICLE INFO

Article history:
Received: 2024-08-15
Received in revised form: 2025-10-18
Accepted: 2024-11-01
Published online: 2024-11-01

Keywords: *Spiral heat exchanger; Fouling; Temperature distribution; Optimization; Genetic algorithm*

DOI: *10.22111/cpd.2025.49578.1038*

ABSTRACT

This study presents a novel approach to optimize the thermal design of spiral plate heat exchangers (SPHEs) through a multi-objective genetic algorithm (GA) using MATLAB programming. SPHEs, known for their low fouling and ease of descaling, often outperform conventional heat exchangers for fouling-causing processes. The scientific innovation of this work includes using GA to simultaneously optimize the construction cost and pressure drop while increasing the thermal efficiency by fine-tuning key geometric parameters, including channel spacing and width, hydraulic diameter, and outer diameter. For this purpose, a robust numerical model relying on energy balance equations was introduced to accurately predict the temperature distribution and calculate the total convective heat transfer coefficient (HTC) and logarithmic mean temperature difference (LMTD). The GA-based optimization resulted in a 60% increase in HTC and a 50% reduction in total costs compared to the baseline design. The results confirm the effectiveness of the multi-objective GA method as a powerful optimization tool, indicating strong agreement between the optimized calculations and the SPHE design formulas. This dual improvement in thermal efficiency and cost reduction highlights the practical and economic importance of the proposed method for industrial-scale heat exchanger applications.

1. Introduction

Spiral heat exchangers (SHEs) are widely used for efficient heat exchange between two or more fluids in various applications, including power plants and industrial processes, and also fouling reduction. Compact heat exchangers have recently been extensively studied due to their ideal efficiency [1]. Spiral plate heat exchangers (SPHEs), also known as spiral heat exchangers (SHEs), consist of two flow channels arranged in a spiral to produce first and second

Corresponding author. Tel: +989171613908
E-mail address: khorshidi@hormozgan.ac.ir (J. Khorshidi).

flow channels for the passage of the first (hot/cold) and second (hot/cold) fluids, respectively, similar to the model presented by Nuntaphan [2].

SHEs can properly cool slurries and fluids with high viscosity, distinguishing this type of heat exchanger [3] and justifying its wide applications in various fields such as sugar, paper, and chemical industries for liquid condensation or evaporation [4]. The temperature of the liquid flow during operation is significantly important due to its economic impact. In other words, the evaporation of water from the feed by SHE reduces protein degradation and stimulates microbial stability, thereby reducing capacity and transportation costs. Evaporation and dehydration are two important issues in dairy farming. SHEs can handle highly viscous fluids with poor sedimentation tendency [3]. The geometric configuration of an SHE consists of two long plates, twisted together in a spiral or helical manner. The mechanical quality of the plates is enhanced by welding them with grooves placed in between [5], providing a uniform direction through which local turbulence change can eliminate stagnant zones and lead to self-cleaning flow passage [3].

Kapatkat and Kondhalkar developed an oil extraction system with a spiral tube to reduce costs [6]. Naphon investigated the pressure decline and thermal performance reported for a spiral coil heat exchanger and concluded that the mass flow rate (MFR) of the hot and cold fluids significantly affected the heat exchangers' performance [7]. The design of an SHE was investigated by Nueza et al., who reported a relatively higher heat transfer rate (HTR) for an SPHE than its counterparts [5]. Egner and Burmeister investigated the flow behavior across spiral channels with rectangular cross-sections using computational fluid dynamics (CFD) and revealed the possibility of establishing Nusselt number equations as the spiral's mean diameter function. Furthermore, the most severe heat transfer coefficient (HTC) could be observed in the spiral section. On the other hand, the HTC was almost constant after the arrival time. The flow across spiral channels or channels in laminar flows showed the most significant contribution to the estimation of the heat input length [8, 9]. In addition, an approximate solution was developed to investigate the thermal effect of SHEs in thermal units. Heat exchanger optimization contributes to the most vital areas in thermal designs, carried out through various methods ranging from classical strategies (e.g., Lagrangian coefficient programming, dynamic, geometric, and nonlinear) to non-classical strategies (e.g., discrete maximum random search and principled). A detailed review of the distinct techniques for the optimal design of heat exchangers has been presented up to the 1990s, with their limitations and merits. Minton developed correlations to determine HTC and pressure drop in the calm and turbulent regimes [10, 11].

Martin then extended these equations for pressure drop by considering the fluid friction coefficient [8]. Another research used a code to optimize a new empirical equation of the Nusselt number for SHEs. Various experiments were conducted to measure the performance parameters of the heat exchanger. The code was written to discover new optimized correlations that enabled a valid approximation of the Nusselt number relying on the empirical data provided by 51 experiments. This correlation seemed to have an advantage at low Reynolds numbers. However, in this work, the equation was calculated by considering both sides simultaneously. Considering the experimental data, the overall calculated HTC was within 3.65% of the mean error for the presented correlation. As shown by the full uncertainty analysis, the results of the new correlation of Nusselt number were within ±3% of the true Nusselt number [12]. Among the various heat exchangers, SPHE has a significant place in the fluid cooling and heating industries. According to Fig. 1, this heat exchanger consists of two flat plates, wrapped around a rod or tube, and two coaxial

channels, separately sealed on both sides at the ends of the channels by welding a plate to prevent mixing of the two fluids. A hinged cover with a gasket is used on each side of the SHE. The heat exchanger's interior and the heat transfer surfaces on both the cold and hot sides can be accessed by opening the designed covers [13]. The production and application of these heat exchangers began in the 1990s in the cellulose industry and expanded to various fields. However, compared to their counterparts, these heat exchangers have been less evaluated theoretically and experimentally (Fig.1).

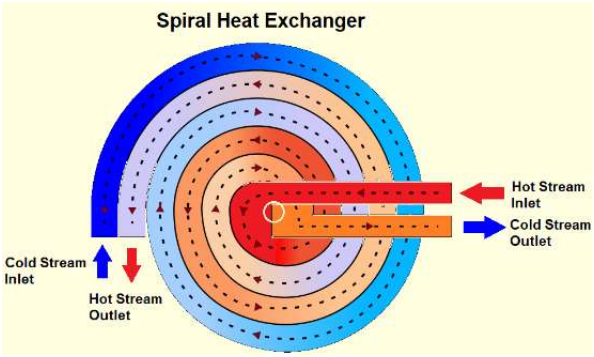

Fig 1. Flow pattern and geometry of an SHE [14]

Minton presented the first equations for the total heat transfer factor and pressure drop estimations under different application modes [15].

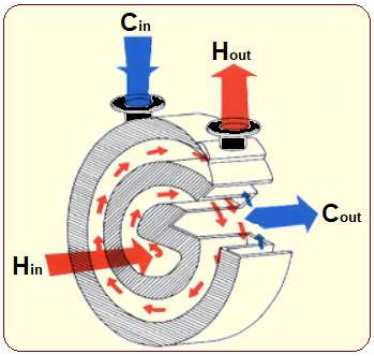

Fig.2. Geometric configuration of the SPHE channel and represented model parameters [20]

Other studies have simultaneously sought to highlight the relationship between heat transfer and pressure drop. Heat exchanger designers have examined the temperature distribution across the length of the heat exchanger, mostly following two professors at the University of Hamburg, Bes and Rotzel [16-19]. This heat exchanger can be easily cleaned and descaled due to the ease of access to all its surfaces. The temperature correction factor is very close to 1, resulting in the high thermal efficiency of the SHE [20].

Recent advances in optimization methods have focused on enhancing heat transfer and reducing cost by integrating computational techniques. Jiang et al. investigated the structural optimization of spiral fin and tube heat exchangers using numerical simulations and support vector regression to identify key geometric parameters that maximize heat transfer while minimizing thermal resistance. Their multi-objective optimization approach significantly improved performance indices, validating the method for practical use in industrial applications [21]. Similarly, Bidabadi et al. [22] employed a genetic algorithm (GA) for SPHE optimization, seeking to balance the improvement of convective

HTC and the reduction of pressure decline. The results showed a 13% improvement in HTC and a 50% reduction in total costs compared to the baseline designs, indicating the effectiveness of GA in the construction management of a converter based on optimal economic and thermodynamic parameters.

Furthermore, Bidabadi et al. [23] highlighted the role of GA-based optimization in the design of compact heat exchangers with rational constraints. They achieved a 60% improvement in HTC while reducing costs by 20% by simultaneously optimizing geometric variables such as channel spacing and width, further emphasizing the contribution of GA to high-efficiency and cost-effective heat exchanger designs.

Collectively, these studies demonstrate that advanced optimization algorithms such as GA can provide robust solutions for SPHE design improvement. The integration of numerical analysis and machine learning tools has further expanded the scope of optimization, enabling precise control over geometric and operational parameters to meet modern energy consumption requirements. Unlike previous studies, this research introduces a comprehensive, multi-objective optimization framework that simultaneously modifies key SPHE geometric parameters, channel spacing, width, hydraulic diameter, and external diameter to improve heat exchanger performance. The novelty lies in integrating energy balance equations into GA-based optimization to accurately model temperature distribution and HTC while minimizing pressure drop and costs. It is worth noting that a 60% improvement in HTC and a 50% reduction in costs can be achieved in the proposed optimization framework, surpassing previous benchmarks. This study presents a valid and robust design method that bridges the gap between numerical modeling and practical feasibility, significantly contributing to heat exchanger optimization.

The current work has modeled a spiral heat exchanger using some mathematical relations. Some calculation methods are employed for the optimization of the cost and thermal design by MATLAB programming, eventually seeking to find optimized parameters by Genetic Algorithm (GA) to minimize SHE's cost and size.

2. Methodology

The current work has employed a multi-objective genetic algorithm (MOGA) to implement the optimization process, where an SHE was selected from a primary population of randomly generated individuals characterizing potential solutions. The GA utilizes the idea of the fittest survival to generate more desirable individuals in the population's successive evolutionary generations. The more fit individuals are randomly selected from the existing population, and each person's genome is altered (recombined, altered, and sometimes randomly mutated) to progress to a new generation. The following algorithm iteration then uses the fresh batch of potential solutions.

The algorithm usually ends by achieving a maximum number of generations. MOGA uses a set of operators applicable to a population and operates on the population through them. By default, the first population is created at random. This algorithm uses MATLAB Genetic commands and functions to execute the optimized program. This work has been conducted through three separate steps.

1. Identifying overall HTC magnitude by mathematical modeling;
2. Finding an appropriate function for cost and size calculations; and
3. Optimizing the length and price of an SHE by objective function minimization using GA.

The heat exchanger's design is influenced by its applications, including reduction of total cost, HTC, or both. The development of multi-objective and weighted function optimizations, employing GA, would ensure obtaining several

geometric design parameters, securing the minimum pressure decline and maximum overall HTC. Fig. 3 shows the main GA components for implementation in a mathematical problem to optimize parameters.

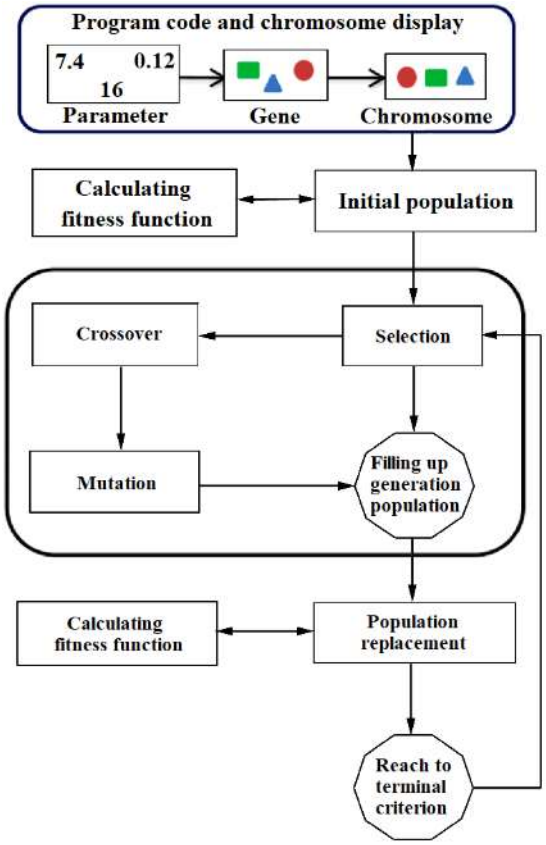

Fig. 3. Block diagram representation of genetic algorithms (GAs) [22]

3. Mathematical formulations

3.1. Governing for heat transfer

The Overall HTC relates HTR to the temperature differences within the fluid and has general applications in the heat exchangers' design. It covers all the HTR resistances, comprising cold and host fluid films, wall thickness, and sediment resistance on the hot and cold streams. The heat transfer equation is presented as follows [1, 24, 26]:

$$Q = \dot{m}_h C_h (T_{hi} - T_{ho}) = \dot{m}_c C_c (T_{ci} - T_{co}) \tag{1}$$

The physical principle relies on energy conservation, *i.e.*, the hot stream's heat loss equals the cold stream's heat gain, assuming insignificant heat loss to the surroundings. The total heat load on the heat exchanger has been evaluated in this study using the thermal equilibrium equation. Logarithmic mean temperature difference (LMTD) contributes critically to the overall HTC assessment under pre-defined temperatures at the inlet and outlet [1, 26]. The heat duty can be determined by:

$$Q = U.A.LMTD \tag{2}$$

In the above equation, A shows the heat transfer area, while F denotes the correction factor and the hot-cold fluid LMTD. The overall HTC is also obtained through the following equation:

$$U = \frac{1}{\frac{1}{h_h} + \frac{t_w}{K_w} + \frac{1}{h_c} + R_f} \tag{3}$$

where h_h, h_c, represent the convection HTCs associated with hot and cold fluids, respectively. K_w represents the wall material's conductivity, while R_f stands for the fouling factor. Besides, t_w is the wall thickness, and h_h and h_c can be determined by experimental relations for the spiral heat transfer [1, 23]. The LMTD is close to 1 in this heat exchanger. Meanwhile, the flow in this heat exchanger resembles the actual reverse flow. The above heat exchanger also shows a much bigger overall HTC than the values reported for the shell and tube heat exchangers, implying the SHE's small size [24]. LMTD can be determined by Eq. (4) [1, 26].

$$LMTD = \frac{(T_{hi} - T_{co}) - (T_{ho} - T_{ci})}{\ln(\frac{T_{hi} - T_{co}}{T_{ho} - T_{ci}})} \tag{4}$$

The expressions below are employed for the heat transfer area and Nusselt number estimations:

$$A = 2 \times L \times H \tag{5}$$

$$Nu = 0.239(1 + 5.54\frac{D_H}{R_m})\mathrm{Re}^{0.806}\,\mathrm{Pr}^{0.268} \tag{6}$$

Nusselt number is determined using Eq. (6). Having the Nusselt number from the Reynolds and Prandtl numbers, the HTC can be evaluated using Eq. (6). Here, D_H and R_m represent the heat exchanger's hydraulic and mean diameters, respectively. The Reynolds number can be expressed considering mass flux (M), as shown in the following:

$$\mathrm{Re} = M.\frac{D_H}{\mu} \tag{7}$$

Eqs. (8) and (11) can be utilized in the above equation to determine the mean fluid velocity (v) and Prandtl number (Pr), in which ρ, $\dot{m}$, and k denote the fluid density, mass flow rate, and thermal conductivity, respectively [1, 25].

$$\nu = \frac{\dot{m}}{\rho A} \tag{8}$$

$$M = \frac{m}{A_c} \tag{9}$$

The mean radius is calculated as follows:

$$R_m = \frac{R_{\min} + R_{\max}}{2} \tag{10}$$

Prandtl number can be evaluated based on the physical properties of the stream through the equation below.

$$\mathrm{Pr} = \frac{C_p \mu}{k} \tag{11}$$

Estimating the Nusselt number from the Reynolds and Prandtl numbers, the HTC can be obtained through the following:

$$h = \frac{k.Nu}{D_H} \tag{12}$$

3.2. Pressure drop in SPHE

Pressure drop is obtained through the following equation in SHEs' streams and external diameter [1, 25].

$$\Delta P = \frac{1.45(L.v^2\rho)}{1.705} \tag{13}$$

where, v shows the velocity, and ρ is the density of the fluid.

3.3. Cost estimation

The total cost was determined as the sum of the manufacturing cost (C_i) and operational cost (C_{od}) [1, 25].

$$C_{total} = C_i + C_{od} \tag{14}$$

The heat exchanger's surface influences manufacturing cost (C_i), according to the Hall equation [1, 25].

$$C_i = e_1 A^j \tag{15}$$

Here, e_1 = 5973 and j =0.59, as presented in the operational costs [22, 25]:

$$C_{od} = \sum_{k=1}^{ny} \frac{C_o}{(1+i)^k} \tag{16}$$

$$C_o = P.C_E.Hr \tag{17}$$

$$P = \frac{1}{\eta}\left(\frac{\dot{m}_h}{\rho_h} \times \Delta P_h + \frac{\dot{m}_c}{\rho_c} \times \Delta P_c\right) \tag{18}$$

Table1, provides additional information required for the operating cost and HTC calculation.

Table 1. Further parametric information required for the optimization process [25]

Parameters	Symbols	Values	Units
Number of years	*ny*	15	years
Annual discount rate	*i*	0.1 (10%)	-
Energy cost	C_E	0.00012	(Euros/w.hr)
Annual work hours	*Hr*	8000	(hr/year)
Pumping efficiency	η	75%	-

4. Problem description

4.1. Design procedur

An SPHE was modeled considering the fluid flow and heat transfer properties and the stated hot and cold flow rates. MATLAB (R2018a) software was utilized to model optimized SPHE by GA algorithm. The cold and hot fluids had constant inlet temperatures, while their outlet temperatures should be estimated for counter-current arrangement.

Table 2. Specifications of the SPHE

Parameter	Value
Height (plate width) (m)	0.457
Plate length (m)	2.515
Spiral diameter (m)	0.304
Channel spacing (m)	0.00635
Heat transfer area (m^2)	3.49
Plate thickness (m)	0.001
Plate material	Stainless steel
Stainless steel heat conductivity (W/m°C)	14
Number of turns	7

An SHE has been employed to cool the ethylene glycol. The flow rate of ethylene glycol is set to 0.8kg/s, which should be cooled from 80°C. The water-cooling fluid enters the heat exchanger at a 0.5kg/s flow rate, which must be heated from 32.87°C. The fouling factor is 0.00017 $m^{2\circ}$C/W. The heat exchanger's wall is stainless steel.

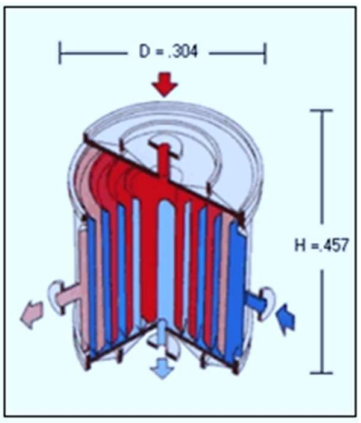

Fig.4. Geometrical features of modeled SPHE [12]

The appropriate heat exchanger is selected considering the physical characteristics of cold and hot fluids, as shown in Fig. 4. The temperature distribution is also checked after designing the heat exchanger.

Table 3. Thermodynamic and physical properties of the streams

Parameter	Cold stream	Hot stream
Working fluid	Water	Nitrobenzene
MFR (kg/s)	0.5	0.8
Inlet Temperature (°C)	32.87	80
Outlet Temperature (°C)	56	36.84
Average balk Temp (°C)	44.43	58.42
Mean wall Temp (°C)	46	60
Specific Heat (J/kg.°C)	4180	1400
Thermal Conductivity (W/m.°C)	0.622	0.149
Specific Gravity	1	1.2
Allowable pressure (kPa)	35	35
Dynamic viscosity (Pa.s) at average balk Temp	0.009	0.00181
Dynamic viscosity (Pa.s) at wall Temp	0.0072	0.0017

The heat exchanger correction factor is about 0.99, and the turbulent flow is considered for hot and cold fluids, through the Reynolds dimensionless number. The hydraulic diameter of an SPHE is given as follows [1]:

$$D_H = \frac{2Hb}{H+b} \tag{19}$$

In which, b shows the channel plate spacing, H denotes the plate height. The Reynolds number is identified by the mass transfer rate for both hot and cold streams [1, 25].

$$\dot{m} = \rho v A_s = \frac{\rho v \pi D_H^2}{4} \tag{20}$$

$$\mathrm{Re}_c = \frac{\rho_c v_c D_H}{\mu_c} = \frac{\dot{m}_c}{4\pi\mu_c D_H} \tag{21}$$

$$\mathrm{Re}_h = \frac{\rho_h v_h D_H}{\mu_h} = \frac{\dot{m}_h}{4\pi\mu_h D_H} \tag{22}$$

where A_s is the surface area of the free flow. As a turbulent flow passes an SPHE, we have to use turbulent flow equations to estimate the heat transfer. Specifically, the Reynolds number ranges from 1412 to 7546 for the cold fluid (Re_c) and 11298 to 60372 for the hot fluid (Re_h), covering both laminar and turbulent flow regimes. This range of Re numbers characterizes the flow conditions in the spiral plate heat exchanger (SPHE) and ensures more convenient repeatability of the study.

4.2. Calculating important parameters

The tube wall temperature is usually 2-3°C higher than the average temperature (T_{avg}) of the passing flow; thus, the viscosity can be well approximated at the average wall temperature (T_w). The Nusselt number and HTC of the hot and cold flows are found in Eqs. (6) and (12) [26]. These calculations involve estimating temperatures and the required thermodynamic parameters. The fluid's average temperature is determined by:

$$T_{avg} = \frac{T_{in} + T_{out}}{2} \tag{23}$$

where, T_{in} and T_{out} show the fluid temperatures at the beginning and end of the process, respectively. Further calculations lead to the HTC estimation. Hence, the area for heat transfer in an SPHE can be calculated by the following [1, 25].

$$A = \frac{Q}{U.LMTD}(m^2) \tag{24}$$

Thus, the spiral plate's optimal length is:

$$L = \frac{A}{2.H}(m) \tag{25}$$

where, H represents SHE's height. The numerically determined length of the spiral plate value properly agrees with its geometrical features.

4.3. Optimization

The present problem ultimately focuses on minimizing the SHE's total cost considering certain constraints and the case investigated by Moretta [4]. The Genetic algorithm 'GA' is applied in MATLAB to compare the results to those of GA and WDO optimizations. The SHE-related total cost comprises the manufacturing and operation costs. As shown, the total capital (C_{total}) is minimized. No constraints are considered in this optimization study. The pressure declines when the fluid flows along hot and cold sides. The pressure drops in the hot and cold flows, and the outer diameter, length, and width of SHE would form the design variables undergoing optimization. Table 4 presents the upper and lower bounds of all the design variables. The hot and cold streams' physical specifications have been taken from Moretta et al. and cross-verified in Bidabadi [1, 4, 22].

Table 4. Variables' lower and upper bounds throughout the optimization calculations [27]

Design variables	Lower bound	Upper bound
Hot fluid pressure drop (Pa.s)	0	40000
Cold fluid Pressure drop (Pa.s)	0	20000
Outer diameter (m)	0.3	1.5
Length (m)	1	2
Width (m)	0.3	2.5

4.4. Optimal design parameters

The enhancement of the SHE depends on its geometrical factors. For example, the plate spacing enhances the pressure drop upon declining the space between the spiral plates, implying the need for higher pumping energy, which can improve the HTC and thermal efficiency of the heat exchanger. The spacing channel alterations result in the heat transfer increment, optimizing the thermal and hydraulic performance. Table 5 lists the recommended plate spacing values based on the plate width.

4.5. Using Genetic algorithm for optimization

The present study has used some optimization techniques based on the genetic algorithm. The total cost of Eq. (14) was taken as the objective function to satisfy the conditions. The total cost represents the sum of operating and capital costs. The optimized length (L) and width (H) play a vital role by affecting the capital cost. The total heat duty (Q) has been constant considering fixed inlet and outlet temperatures. The average hot and cold stream characteristics were employed as shown in the Table.3 (dataset). The optimization finished in the MATLAB programming upon satisfying the criterion 10^{-12}.

Table 5. Recommended plate spacing values for standard plate widths [28]

Plate spacing (m)	Plate width (m)
0.00476	0.101
	0.152
	0.304
	0.304
0.00635	0.457
	0.457
	0.609
	0.609
	0.762
	0.914
	1.219
0.00793	1.524
0.00952	1.778
0.0127	For more than 1.778 m

4.6. Optimization of the cost and length

As described in Table. 6, four cases were selected for the height and distance of the channels in a spiral heat exchanger and underwent optimizations by the genetic algorithm. The best length and optimal cost were obtained by programming in MATLAB software.

Table 6. The selected cases for optimization

Case	Plate spacing (H)	Plate width (b)
1	0.304	0.00476
2	0.457	0.00635
3	1.524	0.00793
4	1.778	0.0254

The MultiObj_GA code optimizes the fitness function as an objective function under nonlinear constraints. The nonlinear constraints are the range of design variables, *i.e.*, MATLAB makes the rows of the matrix c less than zero while executing the algorithm. The C_{eq} matrix is for nonlinear constraints.

The fitness function code is written as a function. The objective function (TF) of the problem involves length and cost minimization. Input variables are entered, considering the relations for the tube length as FF (1) and those for the distance of the cost calculation as FF (2). Exactly the same relations (the TF objective function, including the square root) are calculated. The mentioned objective expression is optimized by the genetic algorithm:

$$TF = \sqrt{FF(1)^2 + FF(2)^2} \tag{26}$$

Minimization of this expression implies minimizing the two FF (1) and FF (2) functions, followed by drawing their values in each program iteration. The MultiObj_GA command first shows a few lines (including a description of the

code and how to enter the Case to the user). According to the case, the user selects the values of *H* and *b* through the switch case algorithm and minimizes the target function by applying constraints. When the run is finished, the algorithm shows the values of the optimized length and cost functions.

4.7. Algorithm of SPHE's thermal design optimization

The genetic algorithm was used for function optimization by the following code in the MATLAB library.

$$x = ga(fun,\ nvars\ ,\ A,\ b,\ Aeq,\ beq,\ lb,\ ub,\ nonlcon) \tag{27}$$

This code can find a local minimum of x, to a special function (fun) in another M.file which contains the main script of the heat transfer optimization by MATLAB, like TF, under nonlinear or linear qualities Aeq*x=beq and A*x ≤ b. Moreover, we can set A=[ ], and b=[ ] with some constrains if there are no linear inequalities. The genetic algorithm assesses the matrix product Aeq*x, as if x is transposed (Aeq*x'). Therefore, lb and ub, are lower and upper bounds on the design variables, respectively, for x, such that a solution can be observed in the lb≤x≤ub range, (Set Aeq=[ ] and beq=[ ] in the absence of linear equalities).

Fig. 5 shows the flowchart of Minton's algorithm for the optimization procedure.

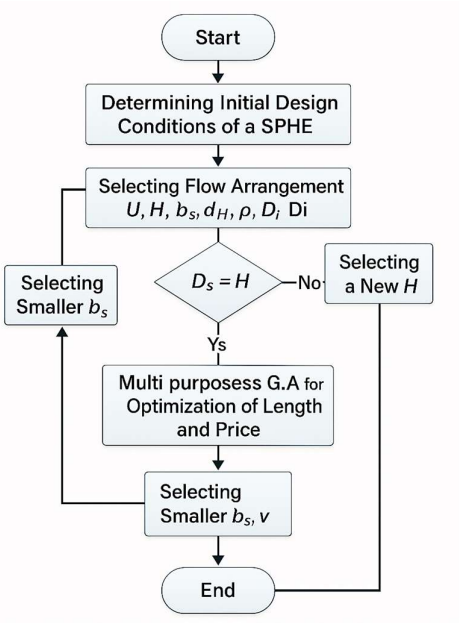

Fig. 5. Simplified flowchart of the developed Minton's algorithm by MATLAB [1]

For the GA optimization process, the following parameters were set in the MATLAB algorithm: population size, mutation rate, and the number of generations were set to 100 individuals, 0.05, and 500, respectively, based on initial experiments and previous studies. These settings could provide a balance between computational efficiency and exploration of a diverse design space. The population size ensures sufficient diversity, while the mutation rate allows for effective exploration without premature convergence [29, 30]. Alternative settings were tested to assess the sensitivity of the results to these parameters. Population sizes and mutation rates at respective ranges of 50-200 and 0.01-0.1 were investigated, revealing that regardless of the relative stability of the optimization performance across these variations, increasing the population size or mutation rate beyond the optimal values resulted in reduced efficiency or excessive computational time. Similarly, the number of generations varied from 200 to 1000, and 500

generations could provide a good trade-off between convergence speed and solution quality. These experiments confirm that the chosen settings were effective and resulted in optimal performance without overfitting or excessive computational costs. The computational burden of the GA optimization process in MATLAB was manageable with a population size of 100, a mutation rate of 0.05, and 500 generations for the study. The total computational time was approximately 1–2hr per optimization run on a computer with moderate processing power (Intel i7 CPU). Despite the moderate computational time, the GA converged efficiently with significant improvements in the objective functions (HTC and cost) observed in the first 200 generations. The convergence speed was constant, showing stable thermal efficiency and cost optimization results.

5. Results and discussion

5.1. The optimization results for the length and construction cost

Table. 7 lists the results of the calculations for various modes. Accordingly, case 2 (H=0.457 m, L=1.281 m) is the most optimal for designing an SHE, as it shows the highest heat transfer and optimal length at the lowest cost. Moreover, case 4 has the minimum pressure drop due to the increment in the cross-section and a decline in the velocity upon enhancement in the heat exchanger's hydraulic diameter. The pressure also decreases by a decrement in the velocity of the fluid. Based on the results, case 4 is not economically suitable, and items 3 and 1 have lower HTCs and higher lengths, respectively.

Table 7. Numerical calculations for SHE's optimization

Parameter	Case. 1	Case. 2	Case. 3	Case. 4
D_H (m)	0.00937	0.0125	0.0158	0.05
Re_c	7546	5647	4483	1412
Re_h	60372	45177	35865	11298
Q (J)	48342	48342	48342	48342
h_h (W/m^2.°C)	27071	16064	10602	1325
h_c (W/m^2.°C)	86358	51244	33823	4229
U (W/m^2.°C)	3448	3094	2737.4	811
A (m^2)	1.051	1.17	1.324	4.467
dp_h (Pa.s)	164690	38290	5155.3	146
dp_c (Pa.s)	77198	17948	2416	68
L (m)	1.728	1.281	0.434	1.256
F (Euros)	6628	6455	7059	14445

Fig. 6 shows a bar graph for different modes of heat exchangers optimized according to Table 6. Case 2 exhibits the lowest construction cost, justifying its selection as the best case. It is also better than cases 1 and 3 due to its great HTC values at the same enthalpy compared to other cases.

The optimal length and cost of the SHE designs were obtained following Minton's model, using the multi-purpose genetic algorithm (multi-objective) and according to the circuit diagram in Fig. 7 derived by MATLAB. The horizontal axis is the number of repetitions in calculations, indicating the ideal length with high precision and up to 120 iterations of the results in a programming loop based on Minton's Algorithm. The optimal cost is also shown using a genetic algorithm program as a MATLAB plot (including key heat transport and fluid mechanic equations, Genetic functions and constraints, boundary conditions, and objective function for cost and length optimization).

Based on Fig. 7, the heat exchanger's optimal length is approximately 1.73m, while the optimal length limit can be chosen between 1.5 and 2m.

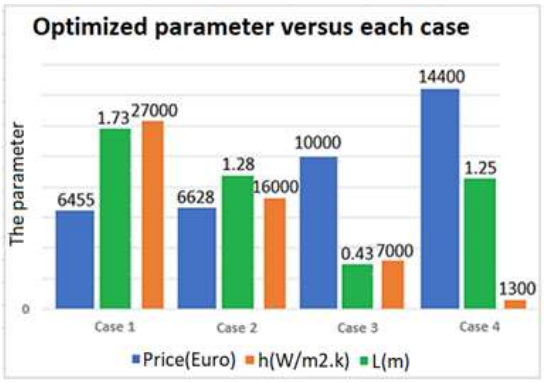

Fig. 6. Bar chart comparing different states of the optimized heat exchanger

According to Fig. 8, the optimal price of the SHE could be around 6455 Euros. The proposed genetic algorithm was performed to minimize the pressure drop within the channels, considering the geometric ratio of the spiral and simultaneously minimizing the total cost. Moreover, the developed Minton algorithm was employed to estimate the design cost and the heat exchanger's length, along with the limiting constraints. The genetic algorithm was utilized to determine the total cost function for four different modes in terms of the SHE's height and length. Accordingly, the highest heat transfer and the optimal length were obtained.

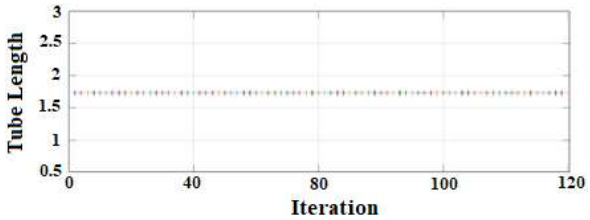

Fig. 7. Calculation of the optimal value of heat exchanger length by GA

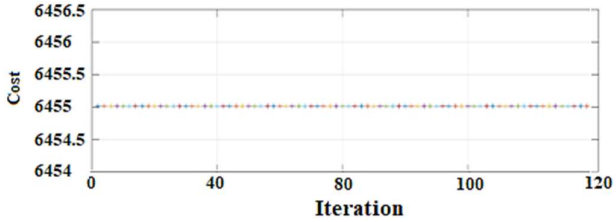

Fig. 8. Calculation of the optimal value of heat exchanger cost by GA

5.2. Temperature distribution throughout the heat exchanger

Fig. 9 depicts the temperature distribution in hot and cold streams passing the SHE per unit length. As seen, the heat flow direction is opposite, the maximum temperature difference occurs at the heat exchanger's beginning, and the hot flow inlet has the maximum inlet temperature.

Therefore, a minimum temperature difference (ΔT_{min}) can be detected at the inlet of the pipe carrying the cold stream (32.86°C) and the outlet of the pipe carrying the hot stream (36.82°C). The optimal length is 1.299m, as shown by analytical solutions. In this study, the temperature distribution in the selected SHE was modeled following energy balance equations that considered both convective heat transfer and fluid thermal resistance. The temperature profile was estimated using the conduction and convection heat transfer equations in the heat exchanger channels,

considering variable flow rates and HTC values along the exchanger. LMTD calculations were used to determine the temperature gradient along the heat exchanger.

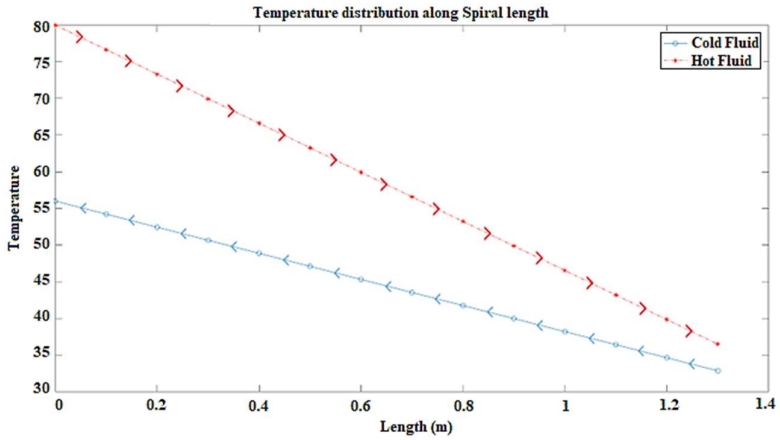

Fig. 9. Cold and hot fluid temperature changes () along the heat exchanger

5.3. Changes in Nu number through spiral heat exchanger

Based on Fig. 10, the hot fluid cools when passing the heat exchanger, and the cold fluid is heated before exiting the heat exchanger. Throughout its path in the heat exchanger, the hot fluid's temperature decreases by 2.5°C every 0.1m, because of which the temperature of the cold stream increases. For both fluids, the Nusselt number rises by enhancing the velocity.

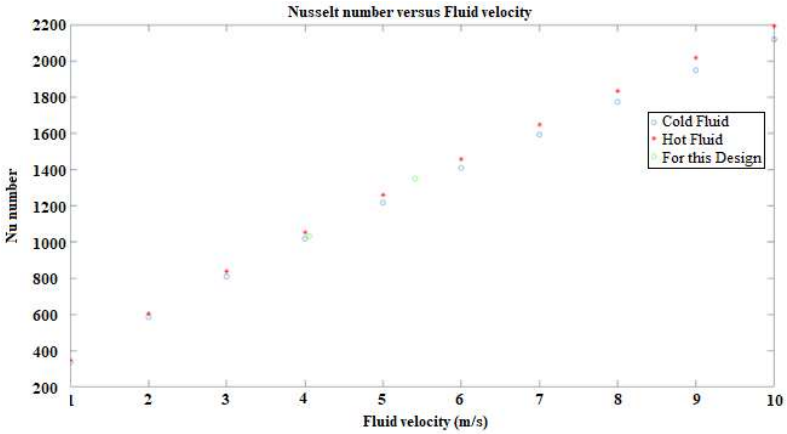

Fig. 10. Variations of Nu number by fluid velocity

The properties of the two fluids are different. Therefore, the Nusselt number of the cold stream will decline if its temperature increases and reaches the hot fluid's temperature.

5.4. Calculation of optimized pressure drop

The optimum pressure drop represents the place with the maximum heat transfer and temperature difference for hot and cold fluids throughout the tube length, *i.e.*, the pipe's first meter and the fluids' minimum speed ($v_{min} \geq 2500*\mu/(\rho.d)$) in the spiral heat exchanger pipe. It also occurs at Re=2500 for turbulent flow. The maximum fluid velocity (v_{max}) is calculated by their mass flow rate (kg/s). Therefore, the optimal speed value lies between these

two values ($v_{min}<v_{opt}<v_{max}$) for both cold and hot flows. The optimal pressure drops within an SHE is determined with a fixed 1.3-m length and a variable length (0-1 m) with a maximum heat transfer rate (ΔT_{max}) (Fig. 9). As the fluids' pressure drop in a heat exchanger is a function of its length and the fluid's velocity, the lower the pressure decline, the higher the heat exchangers efficiency.

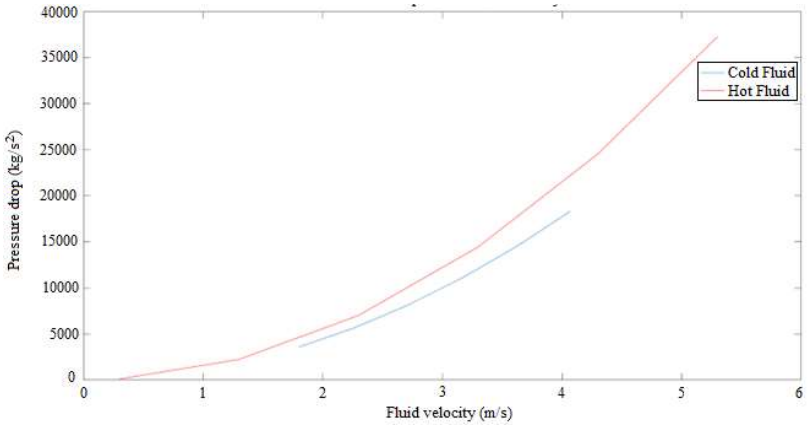

Fig. 11. Pressure drop changes with fluid velocity

According to Fig. 11, the pressure drops increases depending on the fluid velocity, indicating the minimum pressure drop at the slowest fluid velocity. Noteworthy, the SPHE designed by the novel optimization algorithm has lower total costs than the conventional SPHEs. Furthermore, this study used a multi-objective GA that directly considered both heat transfer and pressure drop as competing objectives, allowing the algorithm to find optimal solutions that achieved a balance between these two factors. This approach helps to avoid excessive pressure drop while maintaining optimal heat transfer by fine-tuning the design to meet fluid mechanics and heat transfer requirements. The final optimization design showed a 60% rise in HTC without significantly increasing the pressure drop, confirming the effectiveness of the GA in establishing this balance.

To validate the optimization of heat transfer coefficient (HTC) and manufacturing cost, the optimized GA model (Mintons algorithm) can be compared with traditional baseline designs, such as those proposed by Bidabadi et al. and Moretta, which used conventional design methods based on simplified models and heuristic approaches. These traditional methods have primarily focused on optimizing thermal efficiency or cost but failed to consider these two variables simultaneously. In contrast, the optimized GA model presented in this study considers both objectives, balancing heat transfer efficiency and cost reduction [4, 24].

Quantitatively, optimizations using GA resulted in a 60% increase in HTC compared to conventional designs. Furthermore, the optimized model resulted in a 50% reduction in overall costs compared to the simple and basic design, which showed significant improvements. For example, when using the basic design from Bidabadi et al. [24], the HTC was significantly lower, and the pressure drop was higher, leading to inefficiency in thermal performance. In comparison, the GA-optimized design not only improved the HTC but also reduced the pressure drop, ensuring better flow characteristics without compromising heat transfer [29, 30]. These results demonstrate the advantage of using a multi-objective GA optimization algorithm over traditional methods, which tend to focus only on optimizing a single parameter, without considering the overall trade-off between performance and cost.

In this study, HTC was estimated utilizing the LMTD method and energy balance equations, which account for the variable flow rate and temperature distribution in the SPHE. Specifically, HTC has been derived from the following relationship:

$$HTC = \frac{Q}{A.\Delta T_m} \tag{28}$$

Here, Q, A, and ΔT_{lm} are the heat transfer rate, the heat transfer area, and the LMTD, respectively. To account for fouling, the study introduced a fouling resistance term R_f, which reduces the effective HTC over time. The modified HTC formula is:

$$HTC_{eff} = \frac{1}{\frac{1}{HTC} + R_f} \tag{29}$$

This ensures that the effects of sedimentation are included in the heat transfer. In addition, variable flow rates were considered by adjusting the velocity terms in the flow Reynolds number (Re) and the Nusselt number correlation, allowing the model to account for variations in flow conditions. These adjustments enable the model to capture the effect of different flow regimes (laminar, transitional, and turbulent) and accurately reflect real operating conditions, similar to approaches used in previous studies [21, 29].

6. Conclusion

This paper offers deeper insights into the optimization of spiral plate heat exchangers (SPHEs) using a genetic algorithm (GA) integrated into the MATLAB programming language. The research work focused on designing a cost-effective SPHE configuration that maximized heat transfer while minimizing pressure drop, which was achieved by modifying key geometric parameters such as channel plate spacing, channel width, hydraulic diameter, and external diameter. Through a novel optimization algorithm, this study demonstrated that heat transfer efficiency could be increased while reducing overall costs. Key findings of the study include:

- Optimization and Numerical Analysis: A robust SPHE design was implemented using GA for the spiral heat exchanger.
- Thermal efficiency and cost: The GA-based optimization showed a significant 60% improvement in heat transfer coefficient (HTC) compared to the initial case, along with a 50% reduction in total costs, confirming the economic and operational benefits of the method.
- Parameter effects: The analysis showed that with beneficial geometric and economic considerations, reducing the channel plate spacing and adjusting the channel width and hydraulic and external diameters affected HTC positively and minimized the pressure drop.

The optimized design demonstrated the effective calculation of outlet temperature and HTC based on specific inlet temperatures and flow rates of cold and hot streams, which is crucial for operational efficiency in practical applications. The study confirmed the compatibility between the optimized SPHE length and its geometric dimensions.

In conclusion, this study emphasizes the value of using GA in the SPHE design process to enhance heat transfer and cost efficiency. This method demonstrated the potential of GA as a vital tool in the heat exchangers' optimal design. The optimal parameters identified in this study can significantly contribute to the SHE designs for industrial

applications, as they balance thermal efficiency with cost reduction. Key design elements, such as channel plate spacing, hydraulic diameter, and outer diameter, are scalable for industrial-scale SHEs, designed according to industry standards such as ASTM. Furthermore, the optimization results showed significant improvements in convective heat transfer coefficient (HTC) and cost (60% increase in HTC and 50% decrease in manufacturing costs), which would directly lead to operational benefits in industrial settings, such as improved energy efficiency and lower maintenance costs.

Acknowledgments

This work did not receive any support from any research group. The researchers appreciate the technical support from Seyed Hadi Seyedin.

Nomenclatures

Abbreviation			
ANOVA	Analysis of Variance	T	Temperature (°C)
CHT	Convective Heat Transfer	VIF	Variance Inflation Factor
CI	Confidence Interval	avg	average
DF	Degree of Freedom	c	cold
DOE	Design of Experiment	f	fouling factor
FI	Factor Interaction	h	hot
LMTD	Logarithmic Mean Temperature Difference	i	inlet
RSM	Response Surface Methodology	j	joule
Symbol		m	mass (gr) / meter
A_S	Surface Area	o	outlet
C_p	Heat Capacity ($J \cdot kg^{-1} \cdot K^{-1}$)	s	second
Di	Diameter (inlet/outlet)	w	wall
L	Length of Heat Exchanger	μ	Viscosity ($N \cdot s/m^2$)
M	Mass Flux ($Kg/m^2 \cdot s$)	η	Pumping efficiency (%)
P	Pressure (Pa)	α	alpha (error factor by percentage)
Q	Heat Transfer (J)	n	Pi-Number
R_f	Fouling Resistance	Δ	Delta (Difference)
		ρ	Density (kg/m^3)

References

[1] Sabouri Shirazi, A. H., Jafari Nasr, M. R., Ghodrat, M., 2020. Effects of Temperature Differences in Optimization of Spiral Plate Heat Exchangers. Process Integration and Optimization for Sustainability, 4, 391–408. https://doi.org/10.1007/s41660-020-00128-5

[2] Pradeep Mohan Kumar, K., Vijayan, V., Suresh Kumar, B., Vivek, C. M., Dinesh, S., 2018. Computational Analysis and Optimization of Spiral Plate Heat Exchanger. Journal of Applied Fluid Mechanics, 11 (Special Issue), 121–128. https://doi.org/10.36884/jafm.11.SI.29428

[3] Azad, A. V., Amidpour, M., 2011. Economic Optimization of Shell and Tube Heat Exchanger Based on Constructal Theory. Energy, 36 (2), 1087–1096. https://doi.org/10.1016/j.energy.2010.11.041

[4] Moretta, A. A., 2010. Spiral Plate Heat Exchangers: Sizing Units for Cooling Non-Newtonian Slurries. Chemical Engineering, 117 (5), 44–49.

[5] Picón Núñez, M., Canizalez-Dávalos, G., Martínez-Rodríguez, G., Polley, G., 2007. Shortcut Design Approach for Spiral Heat Exchangers. Food and Bioproducts Processing, 85 (4), 322–327. https://doi.org/10.1205/fbp07040

[6] Kondahkar, G. E., Kapatkat, V. N., 2012. Performance Analysis of Spiral Tube Heat Exchanger Used in Oil Extraction System. International Journal of Modern Engineering Research, 2, 930–936.

[7] Naphon, P., 2007. Thermal Performance and Pressure Drop of the Helical-Coil Heat Exchangers with and without Helically Crimped Fins. International Communications in Heat and Mass Transfer, 34 (3), 321–330. https://doi.org/10.1016/j.icheatmasstransfer.2006.11.002

[8] Egner, M. W., Burmeister, L. C., 2005. Heat Transfer for Laminar Flow in Spiral Ducts of Rectangular Cross Section. Journal of Heat Transfer, 127 (3), 352–356. https://doi.org/10.1115/1.1834624

[9] Burmeister, L. C., 2006. Effectiveness of a Spiral-Plate Heat Exchanger with Equal Capacitance Rates. Journal of Heat Transfer, 128 (3), 295–301. https://doi.org/10.1115/1.2150839

[10] Rao, K. R., 2016. Optimal Synthesis of Shell and Tube Heat Exchangers. Ph.D. Thesis, Indian Institute of Science, Bangalore, India.

[11] Martin, H., 1992. Heat Exchangers. Hemisphere Publishing Corporation, pp.73–82.

[12] Ghodrati, M., Khorshidi, J., 2020. New Experimental Nusselt Number Correlation for Spiral Plate Heat Exchanger Optimized Using a Code. Proceedings of the Institution of Mechanical Engineers, Part A: Journal of Power and Energy, 235 (5), 1142–1151. https://doi.org/10.1177/0957650920948296
[13] Wu, D., 2003. Geometrical Calculations for Spiral Heat Exchangers. Chemical Engineering & Technology, 26 (5), 592–598. https://doi.org/10.1002/ceat.200390091
[14] Fan, Y., Luo, L., Flamant, G., 2013. Design of Compact Heat Exchangers for Transfer Intensification. In: Heat and Mass Transfer Intensification and Shape Optimization, pp. 81–111. https://doi.org/10.1007/978-1-4471-4742-8_4
[15] Minton, P. E., 1970. Designing Spiral Heat Exchangers. Chemical Engineering, May (4), 103–112.
[16] Bes, T., 2001. Thermal Design of Spiral Heat Exchanger. International Journal of Heat Exchangers, 2.
[17] Bes, T., Poetzel, W., 1992. Distribution of Heat Flux Density in Spiral Heat Exchangers. International Journal of Heat and Mass Transfer, 35 (6), 1331–1347. https://doi.org/10.1016/0017-9310(92)90027-5
[18] Bes, T., Roetzel, W., 1998. Effectiveness of Spiral Heat Exchanger with Variable Overall Heat Transfer Coefficient. 7th International Symposium on Heat Exchange and Renewable Energy Sources.
[19] Bes, T., Rotzel, N., 1993. Thermal Theory of the Spiral Heat Exchanger. International Journal of Heat and Mass Transfer, 36 (3), 765–773. https://doi.org/10.1016/0017-9310(93)80043-2
[20] Červenka, B., Holubčík, M., Drga, J., Malcho, M., 2022. Modular Spiral Heat Exchanger Thermal Modelling. Energies, 12 (12), 5805. https://doi.org/10.3390/en12115805
[21] Jiang, H., Jiang, T., Tian, H., Wu, Q., Deng, C., Zhang, R., 2024. Heat Transfer Simulation and Structural Optimization of Spiral Heat Exchangers. Electronics, 13(23), 4639. https://doi.org/10.3390/electronics13234639
[22] Bidabadi, M., Sadaghiani, A.K., Vahdat Azad, A., 2013. Spiral Heat Exchanger Optimization Using Genetic Algorithm. Scientia Iranica, Transactions on Mechanical Engineering (B), 20(5), 1445-1454.
[23] Bidabadi, M., Sadighi Dizaji, H., & Ghasemiasl, R., 2020. A comprehensive analysis for second law attributes of spiral heat exchangers. Applied Thermal Engineering, 174, 115273. https://doi.org/10.1016/j.applthermaleng.2020.115273
[24] Rubenstein, D. A., Frame, M. D., 2022. Mass Transport and Heat Transfer in the Microcirculation. In: Biofluid Mechanics Book (3rd Edition), pp. 331–374.
[25] Anup Kumar, T., Sharma, N., Mohammad, M. N., Pradeep, B. T., Saichand, U., Vamsi, N. M., 2019. Optimization of Spiral Plate Heat Exchanger by Gradient Based Optimizer. International Journal of Innovative Technology and Exploring Engineering (IJITEE), 8 (6), 2278–3075.
[26] Patel, A., Boersma, B. J., Pecnik, R., 2016. The Influence of Near-wall Density and Viscosity Gradients on Turbulence in Channel Flows. Journal of Fluid Mechanics, 809, 793–820. https://doi.org/10.1017/jfm.2016.662
[27] Chowdhury, K., Linkmeyer, M., Bassiouny, K., 1990. Analytical Studies on the Temperature Distribution in Spiral Plate Heat Exchangers: Straightforward Design Formulae for Efficiency and Mean Temperature Difference. Chemical Engineering and Processing, 19, 183–190. https://doi.org/10.1016/0255-2701(84)80020-3
[28] Canizalez Dávalos, L., Murrieta Luna, E., Rodríguez Ángeles, M. A., Cruz Delgado, V. J., 2019. Designing Spiral Plate Heat Exchangers to Extend Its Service and Enhance the Thermal and Hydraulic Performance. In: Low-temperature Technologies Book, Edited Volume. https://doi.org/10.5772/intechopen.85345
[29] Zhao, C., Liu, B., Piao, S., Wang, X., et al., 2017. Temperature Increase Reduces Global Yields of Major Crops in Four Independent Estimates. Proceedings of the National Academy of Sciences of the United States of America, 114 (35), 9326–9331. https://doi.org/10.1073/pnas.1701762114
[30] Zhang, X., Wang, L., Zhang, Y., 2021. Performance Optimization of the Helical Heat Exchanger with Fin. Frontiers in Energy Research, 9, 789316. https://doi.org/10.3389/fenrg.2021.789316